

# UCSF

## UC San Francisco Previously Published Works

### Title

Changes in arginase isoforms in a murine model of neonatal brain hypoxia-ischemia.

### Permalink

<https://escholarship.org/uc/item/42r0x198>

### Journal

Pediatric research, 89(4)

### ISSN

0031-3998

### Authors

Mike, Jana K  
Pathipati, Praneeti  
Sheldon, R Ann  
et al.

### Publication Date

2021-03-01

### DOI

10.1038/s41390-020-0978-3

Peer reviewed



## BASIC SCIENCE ARTICLE

# Changes in arginase isoforms in a murine model of neonatal brain hypoxia–ischemia

Jana K. Mike<sup>1</sup>, Praneeti Pathipati<sup>1</sup>, R. Ann Sheldon<sup>2</sup> and Donna M. Ferriero<sup>1,2</sup>

**BACKGROUND:** Arginases (ARG isoforms, ARG-1/ARG-2) are key regulatory enzymes of inflammation and tissue repair; however, their role after neonatal brain hypoxia (H) and hypoxia–ischemia (HI) remains unknown.

**METHODS:** C57BL/6 mice subjected to the Vannucci procedure on postnatal day (P9) were sacrificed at different timepoints. The degree of brain damage was assessed histologically. ARG spatiotemporal localization was determined via immunohistochemistry. ARG expression was measured by Western blot and activity spectrophotometrically.

**RESULTS:** ARG isoform expression increased during neurodevelopment (P9–P17) in the cortex and hippocampus. This was suppressed with H and HI only in the hippocampus. In the cortex, both isoforms increased with H alone and only ARG-2 increased with HI at 3 days. ARG activity during neurodevelopment remained unchanged, but increased at 1 day with H and not HI. ARG-1 localized with microglia at the injury site as early as 4 h after injury, while ARG-2 localized with neurons.

**CONCLUSIONS:** ARG isoform expression increases with age from P9 to P17, but is suppressed by injury specifically in the hippocampus and not in the cortex. Both levels and activity of ARG isoforms increase with H, while ARG-1 immunolabelling is upregulated in the HI cortex. Evidently, ARG isoforms in the brain differ in spatiotemporal localization, expression, and activity during neurodevelopment and after injury.

*Pediatric Research* \_\_\_\_\_; <https://doi.org/10.1038/s41390-020-0978-3>

### IMPACT:

- Arginase isoforms change during neurodevelopment and after neonatal brain HI.
- This is the first study investigating the key enzymes of inflammation and tissue repair called arginases following murine neonatal brain HI.
- The highly region- and cell-specific expression suggests the possibility of specific functions of arginases.
- ARG-1 in microglia at the injury site may regulate neuroinflammation, while ARG-2 in neurons of developmental structures may impact neurodevelopment.
- While further studies are needed to describe the exact role of ARGs after neonatal brain HI, our study adds valuable data on anatomical localization and expression of ARGs in brain during development and after stroke.

## INTRODUCTION

A critical determinant of neuronal survival after brain hypoxia–ischemia (HI) is neuroinflammation, resulting from mechanisms of oxidant stress, inflammation, and excitotoxicity. The neonatal brain has a low antioxidant reserve; therefore, oxidative stress such as that from excess nitric oxide (NO) may lead to neuroinflammation, neuronal death, and poor clinical outcomes.<sup>1</sup>

The key regulatory enzymes of inflammation and tissue repair are arginases (ARGs), which are expressed in two isoforms: ARG-1 predominantly found in the liver and lung, and the more recently discovered ARG-2, confined mainly to the kidney, brain, prostate, and pancreas.<sup>2</sup> ARGs are generally described as urea cycle enzymes, and recent findings suggest that the complete urea cycle could also occur in the brain<sup>3</sup> and play a role in disease.<sup>4–6</sup> As ARG regulate NO synthesis via competition for the common

substrate arginine<sup>7</sup> (NO pathway), they are capable of regulating the acute phase of inflammation through processes such as oxidative stress,<sup>8</sup> apoptosis,<sup>9</sup> or microglia polarization.<sup>10</sup> Additionally, certain products of the ARG metabolic pathways (such as polyamines via a polyamine pathway) are essential for cell proliferation and collagen formation,<sup>11</sup> with predicted roles in neuronal growth,<sup>12</sup> axonal regeneration,<sup>13</sup> and glial scar formation.<sup>14</sup> Consequently, ARG clearly impact neurodevelopment as well as processes after brain injury.<sup>15</sup> The ability to regulate NO and polyamine synthesis gives the ARG pathway the potential to serve in new therapies of brain injury, and recent findings in this field have reflected this. The number of studies describing a new role for ARG in various conditions is growing, and a role for ARG has already been recognized in adult brain pathologies, such as inflammation after traumatic brain injury<sup>4</sup> and autoimmune encephalitis.<sup>5</sup> Recently, increased ARG-1 was reported in the

<sup>1</sup>Department of Pediatrics, University of California San Francisco, San Francisco, CA, USA and <sup>2</sup>Department of Neurology, University of California San Francisco, San Francisco, CA, USA

Correspondence: Jana K. Mike (jana.krystofova@ucsf.edu)

Received: 6 November 2019 Revised: 27 April 2020 Accepted: 12 May 2020

Published online: 28 May 2020

blood of stroke patients with levels correlating with infarct size,<sup>6</sup> suggesting the involvement of ARG in post-hypoxic-ischemic mechanisms. So far, many studies suggest ARG-1 as being mostly associated with the role of a marker of “pro-repair” microglia, and ARG-2 mostly in regulation of cerebral blood flow.<sup>15</sup> However, the exact role of ARG remains unclear. While changes in ARG expression and activity have been described in embryonal and adult ages,<sup>16–18</sup> to our knowledge there are very few studies focused on ARG expression and activity during the most robust period of brain development in the postnatal age<sup>15–23</sup> and none after HI injury. Here, we describe for the first time the isoform-specific ARG expression during the postnatal period as a factor in development as well as after HI.

## MATERIALS AND METHODS

### Animals

All animal research was approved by the University of California San Francisco Institutional Animal Care and Use Committee and was performed in accordance with the Guide for the Care and Use of Laboratory Animals. Wild-type mice of the C57BL/6 strain (The Jackson Laboratory, Sacramento, CA) of both sexes were used for all experiments.

### Induction of HI

Neonatal HI was induced in postnatal day9 (P9) mice using the Vannucci procedure. Briefly, unilateral ischemic injury was induced by coagulation of the left common carotid artery under isoflurane anesthesia (4% isoflurane, balance oxygen). The pups were recovered for 1 h with their dam. Global hypoxic injury was triggered by exposure to 50 min of hypoxia in a humidified chamber at 37 °C with 10% oxygen/balance nitrogen. The mice were euthanized at 1 h, 4 h, 12 h, 1 day, 3 days, 5 days, and 8 days after the procedure. Naive and sham mice (N) were used as controls. The contralateral hypoxic hemisphere (H) in injured animals was studied separately as it was exposed to global hypoxia during the Vannucci procedure and hypoxia alone has been shown to be a stimulus for ARG expression.<sup>16</sup> The hypoxic-ischemic hemisphere was exposed to the initial ischemic insult and subsequent global hypoxia.

### Histology and immunohistochemistry

At each specific timepoint, mice were flushed with 8 mL of phosphate-buffered saline (PBS) and perfused with 10 mL of 4% paraformaldehyde in 0.1 M phosphate buffer (pH 7.4). Brains were post fixed in 4% paraformaldehyde overnight and transferred to 30% sucrose till they sank (3 days). Brains were then flash frozen in 2-methyl butane on dry ice and stored at –80 °C. Coronal sections were cut on a cryostat (12-μm-thick serial sections, 120 μm apart). Brain injury was determined in eight coronal sections stained with Cresyl violet using histopathological scoring in a blinded manner. Sections were assessed rostral to caudal. Regions scored included the following: anterior cortex; middle cortex; posterior cortex; anterior, middle, and posterior caudate/striatum; thalamus; hippocampus CA1, CA2, and CA3; and the dentate gyrus. Scores were assigned for each region as follows: 0 = no injury, 1 = minimal cell loss manifested by scattered shrunken neurons and glia, 2 = moderate cell loss with infarction in a columnar distribution in the cortex with concomitant gliosis or the shrunken hippocampus with cell loss throughout the Sommer's sector, and 3 = severe cell loss and gliosis with cystic infarction, for a total score of 0–33.

Double immunofluorescence labeling was performed on brain sections that were defrosted and air dried at room temperature (RT) for 1 h. Following antigen retrieval in 10 mM citrate buffer (pH 6.0) for 3 min at 90.5 °C and a PBS wash, sections were incubated in blocking solution (10% normal donkey serum, 0.3% Triton X-100, and 10 mg/mL of bovine serum albumin in PBS) for 1 h at RT.

Primary antibody incubation was done overnight at 4 °C with rabbit anti-ARG-1 (1:50, #93668, Cell Signaling Technology); rabbit anti-ARG-2 (1:50, #203071, Abcam); mouse anti-NeuN (NeuN) for neurons (1:500, MAB377, MilliporeSigma), goat anti-Iba1 (Iba1) for microglia (1:100, NB100-1028, Novus Biologicals), mouse anti-gial fibrillary acidic protein (GFAP) for astrocytes (1:300, MAB360, MilliporeSigma), and goat anti-oligodendrocyte transcription factor 2 (Olig2) for oligodendrocytes (1:50, AF2418, Novus Biologicals). After three 5-min PBS washes, sections were incubated for 1 h at RT with appropriate secondary antibodies: donkey anti-goat Alexa Fluor 647 (1:100, A21447, Thermo Fisher), donkey anti-mouse Alexa Fluor 568 (1:100, A10037, Thermo Fisher), and donkey anti-rabbit Alexa Fluor 488 (1:100, A21206, Thermo Fisher). For nuclear staining, sections were stained with 4',6-diamino-2-phenylindol for 5 min. Slides were then washed and coverslipped with ProLong Gold antifade (P36930, Invitrogen). Images were taken with a Leica TCS SP5 Spectral Confocal Microscope.

### Western blotting

Brain tissue was dissected on ice and separated into injured cortex and hippocampus from ipsilateral (HI) and contralateral (H) sides. Tissue extracts for Western blot analysis were prepared in RIPA lysis buffer with added protease and phosphatase inhibitors (Thermo Fisher Scientific, Waltham, MA). Protein concentration was determined using the BCA assay (Pierce). Thirty micrograms of protein was separated by Bis-Tris sodium dodecyl sulfate-polyacrylamide gel electrophoresis using 12-well gels (Invitrogen, Carlsbad, CA) and blotted to polyvinylidene difluoride membranes (Bio-Rad, Hercules, CA) at 30 V overnight at 4 °C. After membrane incubation in blocking buffer (1× TBS, 5% nonfat dry milk, and 0.1% Tween-20) for 1 h at RT, the membranes were probed with the following antibodies: rabbit polyclonal anti-ARG-1 antibody and monoclonal anti-ARG-2 antibody (#9819 ARG-1 polyclonal, #5503 ARG-2 monoclonal, Cell Signaling Technology, 1:100 in blocking buffer) and β-actin (A5316 Sigma-Aldrich) overnight at 4 °C. Liver tissue extract was used as an ARG<sup>+</sup> control. Mouse β-actin (Sigma, 1:2000) was used as a loading control. After three washes in TBST, membranes were incubated with anti-rabbit immunoglobulin G-horse radish peroxidase conjugate (Cell Signaling Technology, 1:1000). The signal was visualized with the ECL chemiluminescence system (Amersham, Little Chalfont, UK). Optical densities (ODs) were measured on scanned radiographs using Image Studio Lite (Li-Cor Biosciences, version 5.2.5) and all markers were normalized to β-actin.

### ARG assay

Total ARG activity was determined spectrophotometrically (Quantichrom™ Arginase Assay kit, BioAssay Systems) as per the manufacturer's instructions. Briefly, hippocampal and cortical tissues were dissected on ice, weighed, and processed in Tris-HCl with protease and phosphatase inhibitor mixtures (Sigma-Aldrich) at 10 μL/mg of tissue. Tissue was homogenized with a Dounce tissue homogenizer and centrifuged at 14,000 r.p.m. for 15 min at 4 °C. Supernatant fractions were incubated at 37 °C for 120 min with 10 mM MnCl<sub>2</sub> in ARG buffer to activate the enzyme. The reaction was stopped by adding urea reagent and samples were further incubated for 60 min at RT. Samples were analyzed with a spectrophotometer at 430 nm and ARG activity in brain samples was calculated as U/L (1 U of ARG converts 1 μmol of L-arginine to ornithine and urea per minute at pH 9.5 and 37 °C).

### Microscopy analysis

To define the anatomical localization of ARG-expressing cells, we grossly evaluated all areas of brain from rostral to caudal at ×5 magnification. For final analysis we chose the anatomical areas with ARG<sup>+</sup> cells and compared these to the contralateral side and N (for ARG-1 cortex and striatum, for ARG-2 hippocampus). Confocal-like Z-stacks (×25 oil objective, 10 μm thick, 1 μm Z step)

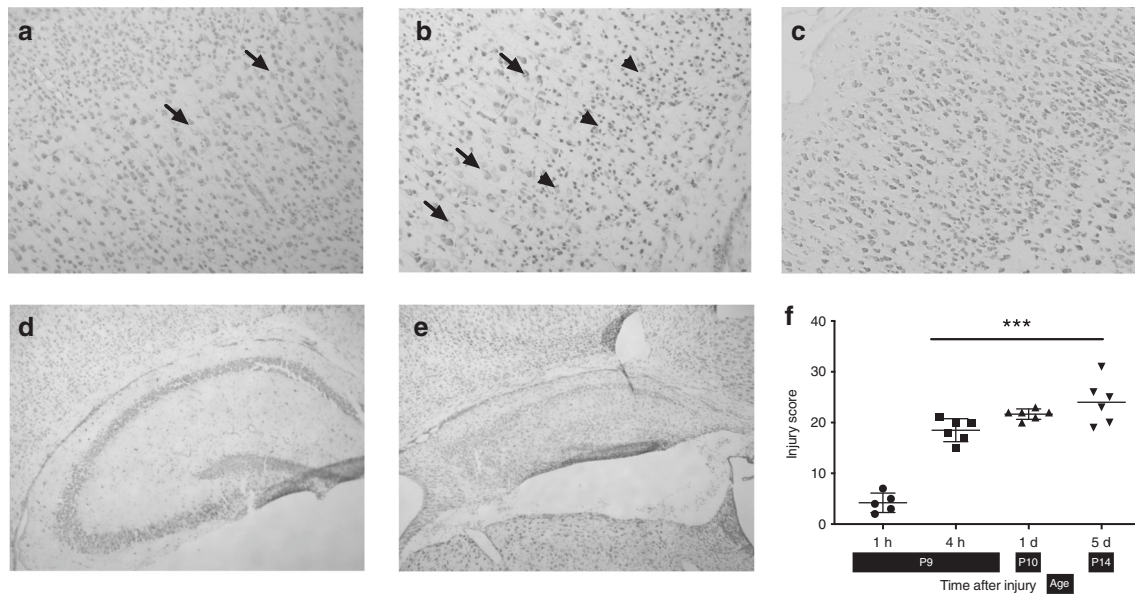


**Fig. 1** Histopathological changes after hypoxic-ischemic brain injury. **a–e** Histopathological analysis of hypoxic-ischemic brain injury at different timepoints: cortex at 1 h (**a**) showing swelling of a few neuronal cells, 4 h (**b**) with increased area of swollen neurons (arrows), pyknotic cells (arrowheads), and 5 days (**c**) after the injury, showing the disruption in cortical structure and cell loss ( $\times 10$  magnification); hippocampus after HI at 4 h with no apparent injury (**d**) and 5 days (**e**) showing injured area with accumulation of shrunken, pyknotic cells, and cystic infarction ( $\times 4$  magnification). **f** Injury scores after HI at different timepoints: injury extends from the cortex at earlier timepoints to involvement of deep brain nuclei and adjacent cortex at the later timepoints. \*\*\* $p < 0.001$ .

were acquired using a Zeiss microscope equipped with the confocal-like optigrid device and Volocity software (Improvision). Analysis was performed in anatomical areas corresponding to slide 66 of the Allen Mouse Brain Atlas.<sup>24</sup> Matching regions of interest ( $500 \times 400 \mu\text{m}^2$ ) in N mice served as a control. Every brain had a control with no primary antibodies for staining. Image capturing (using Volocity software) and analysis (Fiji, ImageJ) was done in a blinded manner. The number of cells that express ARG-1 was quantified manually.

#### Statistical analysis

Analyses were performed using Prism 7 (GraphPad Software, San Diego, CA). All data are shown as mean  $\pm$  SEM. Grouped data were analyzed using two-way analysis of variance and subsequently subjected to Bonferroni  $t$  tests for post hoc analyses and differences were considered significant at  $p < 0.05$ . Comparisons were made between HI, H, and N groups at different timepoints. For Western blot expression data,  $t$  tests were used to compare expression at P9 vs. P17 only for the N animals to clarify the significant changes due to neurodevelopment.

## RESULTS

### Evolution of HI brain injury over time

Brain HI injury evolves over time with corresponding histological changes at different timepoints ranging from 1 h (P9) to 5 days (P14) after the injury (Fig. 1). The early changes that occur within 1 h after the injury are characterized by swelling of cortical neurons seen with cresyl violet stain (Fig. 1a). At later timepoints, the injury spreads from the cortex (Fig. 1b, c) into deeper brain structures such as the hippocampus, thalamus, and striatum (Fig. 1d, e). This pattern corresponds to lower scores in the more immediate period after the injury compared to higher scores at the later timepoints (Fig. 1f).

ARG expression changes during neurodevelopment and as a result of HI

To investigate if ARG expression changes during neurodevelopment and how brain H and HI affect their expression, we

measured the expression of ARG isoforms ARG-1 and ARG-2 in the cortex and hippocampus at different timepoints after the injury using Western blotting.

### ARG-1 expression

There was a developmental increase in ARG-1 expression from P9 to P17 in both regions of N mice (Fig. 2a, b): cortex at P9 ( $n = 13$ ) vs. P17 ( $n = 17$ ), (Fig. 2a,  $p < 0.001$ ), hippocampus at P9 ( $n = 18$ ) vs. P17 ( $n = 14$ ), (Fig. 2b,  $p < 0.0001$ ). Following the Vannucci procedure, ARG-1 expression increased in the H cortex ( $n = 7$ ) 5 days after the injury compared both to the HI cortex ( $n = 7$ ) (Fig. 2a,  $p < 0.0001$ ) and age-matched N mice ( $n = 10$ ), as well as to the H cortex at all other timepoints (Fig. 2a,  $p < 0.0001$ ). Hippocampal expression of ARG-1 was reduced at later timepoints after the injury compared to N age-matched animals ( $n = 10$ – $14$ ) in both H hemisphere ( $n = 7$ – $11$ ) (3 days,  $p = 0.0467$ ; 5 days,  $p = 0.0028$ ; 8 days,  $p < 0.0001$ ) and HI hemisphere (8 days,  $p = 0.0003$ ) (Fig. 2b).

### ARG-2 expression

ARG-2 also exhibited a developmental increase in expression from P9 to P17 in N mice (Fig. 2c, d): cortex at P9 ( $n = 16$ ) vs. P17 ( $n = 17$ ) (Fig. 2c,  $p < 0.001$ ) and hippocampus at P9 ( $n = 18$ ) vs. P17 ( $n = 15$ ) (Fig. 2d,  $p < 0.0001$ ). Following the Vannucci procedure, there was a significant increase in ARG-2 expression in the H cortex at 3 days ( $n = 6$ ;  $p < 0.0001$ ) and 5 days ( $n = 7$ ;  $p < 0.0001$ ) after the injury compared to N age-matched animals ( $n = 10$ – $16$ ). In HI cortex, ARG-2 expression peaked at 3 days after the injury ( $n = 6$ ;  $p < 0.0001$ ) and was suppressed by 5 days ( $n = 7$ ;  $p < 0.0001$ ). Hippocampal expression of ARG-2 peaked transiently in H hemisphere 3 days after the injury ( $n = 6$ ;  $p < 0.001$  vs. all other timepoints in that group) and decreased 5 days ( $n = 7$ ,  $p < 0.001$ ) and 8 days after the injury ( $n = 11$ ;  $p < 0.001$ ). In the HI hemisphere, there was a significant increase after HI by 8 days compared to earlier timepoints from that group ( $n = 6$ ;  $p < 0.001$  vs. 1 h, 4 h, 12 h, and 1 day). However, ARG-2 expression was significantly decreased at 8 days in HI ( $n = 6$ ;  $p < 0.0001$ ), as well as in H ( $n = 11$ ;  $p < 0.0001$ ) hemisphere compared to N age-matched animals ( $n = 14$ – $15$ ,  $p < 0.0001$ ).

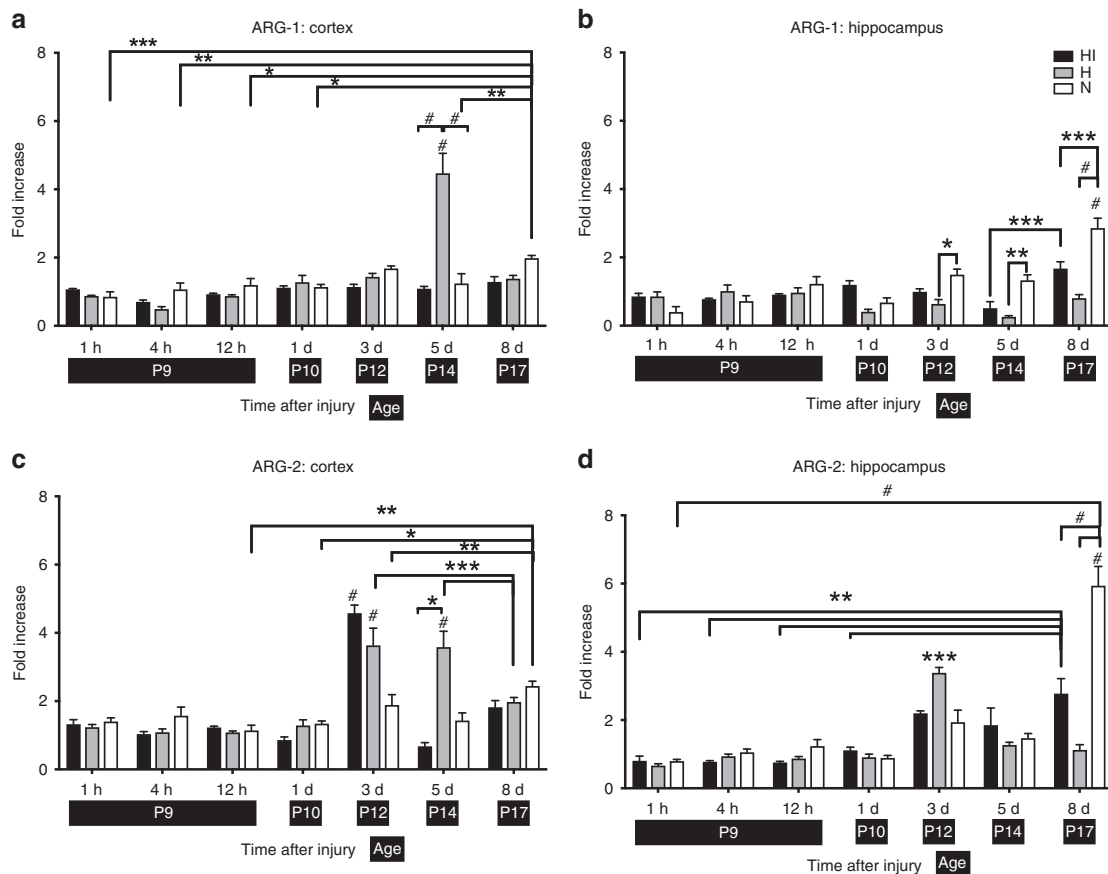


**Fig. 2 Arginase expression in naive mice vs. after brain HI at different timepoints.** Protein expression was measured by Western blotting and presented as the OD ratio to  $\beta$ -actin (for H and HI groups:  $n = 5$  for timepoints 1h, 4h, 12h,  $n = 9-11$  for day 1,  $n = 6-11$  for 3 days,  $n = 7$  for 5 days,  $n = 6-11$  for 8 days after the injury; for N group,  $n = 5-17$  per timepoint). Shown are HI (black), H (gray), and N (white) hemisphere for ARG-1 in the cortex (a) and hippocampus (b) and ARG-2 in the cortex (c) and hippocampus (d). Brackets show significances as follows: \* $p < 0.05$ , \*\* $p < 0.01$ , \*\*\* $p < 0.001$ , and # $p < 0.0001$ . For ARG-1, expression at 5 days in H cortex and expression at 8 days in N hippocampus were both significant against all other timepoints in that group (shown by significance on top of the bar). For ARG-2, expression at 3 days in H and HI cortex, at 3 days in H hippocampus, and 8 days in HI and N hippocampus were significant against all other timepoints in that group (shown by significance on top of the bar).

#### ARG activity is suppressed by HI

As expression of the enzyme may not necessarily translate to its function, we measured ARG activity in N mice and after the Vannucci procedure using a spectrophotometric enzymatic activity measurement kit. As this kit measures the combined activity of ARG and does not separate the activity of ARG-1 and 2, our measures reflected the total ARG activity in the cortex and hippocampus.

Total ARG activity in the cortex and hippocampus was constant postnatally from P9 to P14 and did not differ between the cortex and hippocampus (P9:  $n = 11$  per cortex and hippocampus group,  $p = 0.6063$ , P14:  $n = 8$  per cortex and hippocampus group;  $p = 0.2786$ ) (Fig. 3). There was no significant change in ARG activity in the cortex after the Vannucci procedure ( $n = 7-8$  per HI and H groups,  $n = 6-11$  per N group;  $p > 0.05$ , Fig. 3a). In the hippocampus, however, there was a significant increase in ARG activity 1 day after the injury only in H hemisphere ( $n = 9$  per H group and  $n = 11$  per N group;  $p = 0.0452$ , Fig. 3b).

#### ARG isoforms differ in spatiotemporal expression patterns

**Cellular ARG-1 expression.** Given the changes in ARG expression and activity noted, we wanted to clarify the cell types associated with these changes. Immunofluorescent double-labeling was performed with ARG-1 and either the neuronal marker NeuN, microglial marker Iba1, astroglial marker GFAP, or oligodendrocyte

marker Olig2 (Fig. 4a–d). ARG-1 expression was clearly colocalized only with Iba1<sup>+</sup> cells (Fig. 4b).

Anatomically, ARG-1 was localized with Iba1<sup>+</sup> microglial cells in the areas of olfactory tubercle, pyriform cortex, pallidum, striatum, external capsule of corpus callosum, anterior commissure–temporal limb, amygdala, hypothalamus, and caudate (Fig. 5a). Notably, under normal circumstances in N mice, ARG-1<sup>+</sup>/Iba1<sup>+</sup> cells were absent from the thalamus, hippocampus, internal capsule, and other parts of fiber tracts or cortex at all timepoints studied (P9, P10, P14). After HI, ARG-1<sup>+</sup> microglia morphology was clearly transformed to the amoeboid phenotype at the injury site (Fig. 5b–d) when compared to the ramified phenotype evident in the N mice (Fig. 5e). The changes in ARG-1<sup>+</sup> microglial morphology and accumulation at the injury occurred as early as 4 h after the injury (Fig. 5f–h). At later timepoints, ARG-1<sup>+</sup>/Iba1<sup>+</sup> cell numbers remain elevated both at the HI core in the striatum (24 h:  $n = 6$  per HI and H group,  $n = 8$  per N group; 5 days:  $n = 6$  per HI and H group,  $n = 14$  per N group; 24 h:  $p < 0.0001$  for HI vs. H,  $p < 0.0001$  for HI vs. N; 5 days:  $p < 0.0001$  for HI vs. H and  $p < 0.0001$  for HI vs. N) and the HI hemisphere (24 h:  $p = 0.0025$  for HI vs. H;  $p = 0.0002$  for HI vs. N; 5 days:  $p < 0.0001$  for HI vs. H;  $p < 0.0001$  for HI vs. N) (Fig. 5i, j).

**Cellular ARG-2 expression.** The pattern of ARG-2 expression was noted to colocalize largely to NeuN<sup>+</sup> cells rather than Iba1<sup>+</sup>, GFAP<sup>+</sup>, or



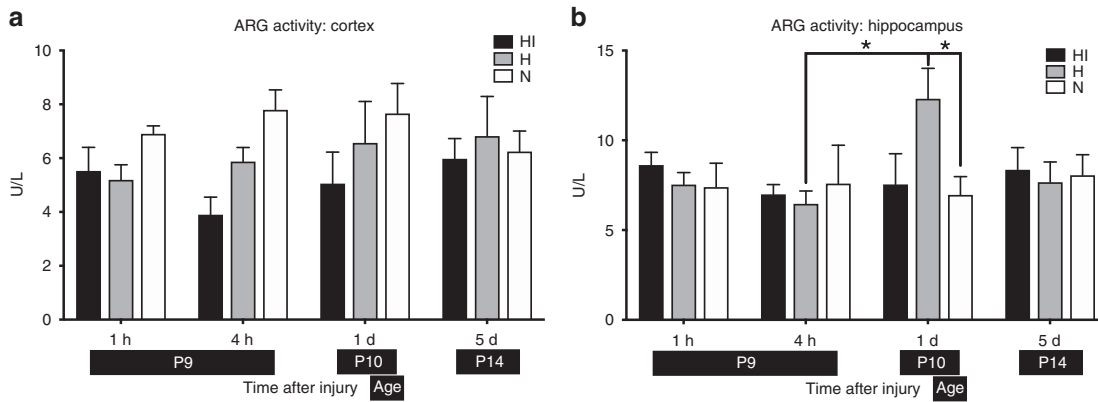


**Fig. 3 Arginase activity in naive mice vs. after brain HI at different timepoints.** Arginase activity in cortex (a) and hippocampus (b) in N mice (white) and in H (gray) and HI hemisphere (black). Unit definition: 1 unit of ARG converts 1  $\mu$ mol of L-arginine to ornithine and urea per minute at pH 9.5 and 37 °C. Brackets show significance with  $*p < 0.05$ .  $n = 7-8$  per HI and H group and  $n = 6-11$  per N group.

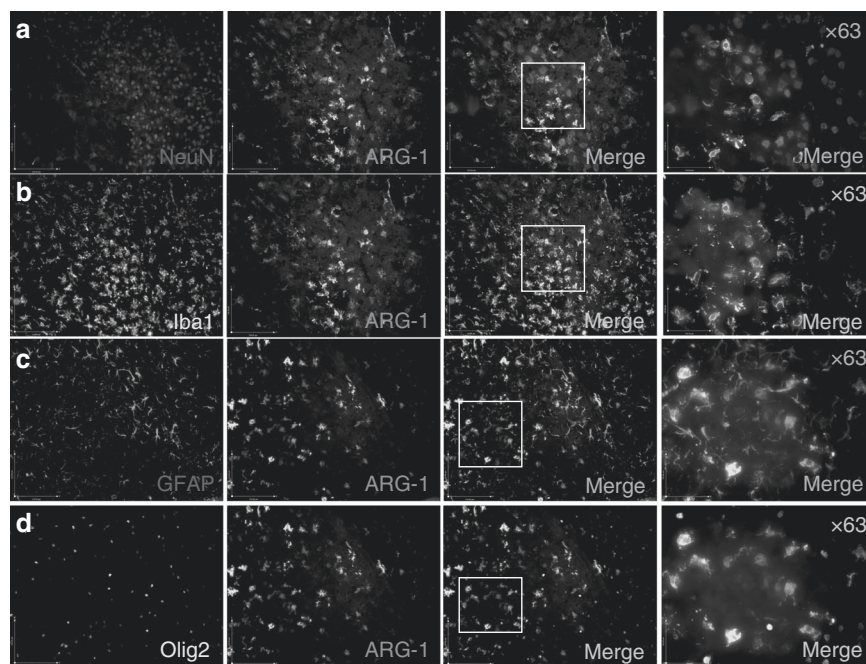


**Fig. 4 Cellular expression of ARG-1.** Images of double immunofluorescent staining with ARG-1 antibody (green, middle panels) paired with an antibody specific for neuron (a: NeuN, red panel), microglia (b: Iba1, cyan panel), astrocyte (c: GFAP, red panel), and oligodendrocyte (d: Olig2, cyan panel). Image  $\times 63$  captures region denoted by a box in the third image of that row. Pictured is the injury site of a P10 mouse exposed to the Vannucci HI model on P9. ARG-1 colocalized with Iba1<sup>+</sup> cells (b).

Olig2<sup>+</sup> cells (Fig. 6a–d). Anatomically, ARG-2 expression was localized in areas of indusium griseum, fasciola cinerea, and CA1 and CA2 of hippocampus, dentate gyrus, and M1 area of the neocortex (Fig. 6e–j). Following HI, ARG-2-expressing cells appeared to have an altered morphology consistent with being injured, in that they appeared pyknotic and shrunken (Fig. 6f, g).

## DISCUSSION

In this study, we elucidate, for the first time, alterations that occur in ARG expression and activity during development from P9 to P14–P17, as well as after H and HI injury. We found that the expression of ARG-1 and -2 increases significantly with age in both the cortex and hippocampus. The expression of ARG-1 and -2 after injury appear to be intrinsically modulated by H alone or HI. Total ARG activity is only modulated by H alone. On the cellular level, both ARG isoforms have very specific expression patterns with

ARG-1 expression predominantly microglial and ARG-2 largely neuronal, both before and after HI. The highly region- and cell-specific expression suggests the possibility of specific functions of ARG isoforms in the brain under physiological and pathological conditions.

While ARG expression has been described in embryonic and very early postnatal (E13–P1),<sup>16,17</sup> young (4 months) and aged (24 months) brains in rat,<sup>18</sup> to the best of our knowledge this study is the first to describe isoform-specific ARG expression patterns during the early postnatal period P9–P17 in mice. We show that ARG-1 expression increases during normal neurodevelopment from neonatal (P9) to infantile age (P17) and is predominantly localized to microglia. Our findings are consistent with Crain et al.,<sup>19</sup> who studied ARG-1 expression exclusively in microglia and detected high messenger RNA expression for the ARG-1 gene in the early postnatal period (P3) that diminished by 70% at P21 and by 90% at 12 months. Similar to ARG-1, we

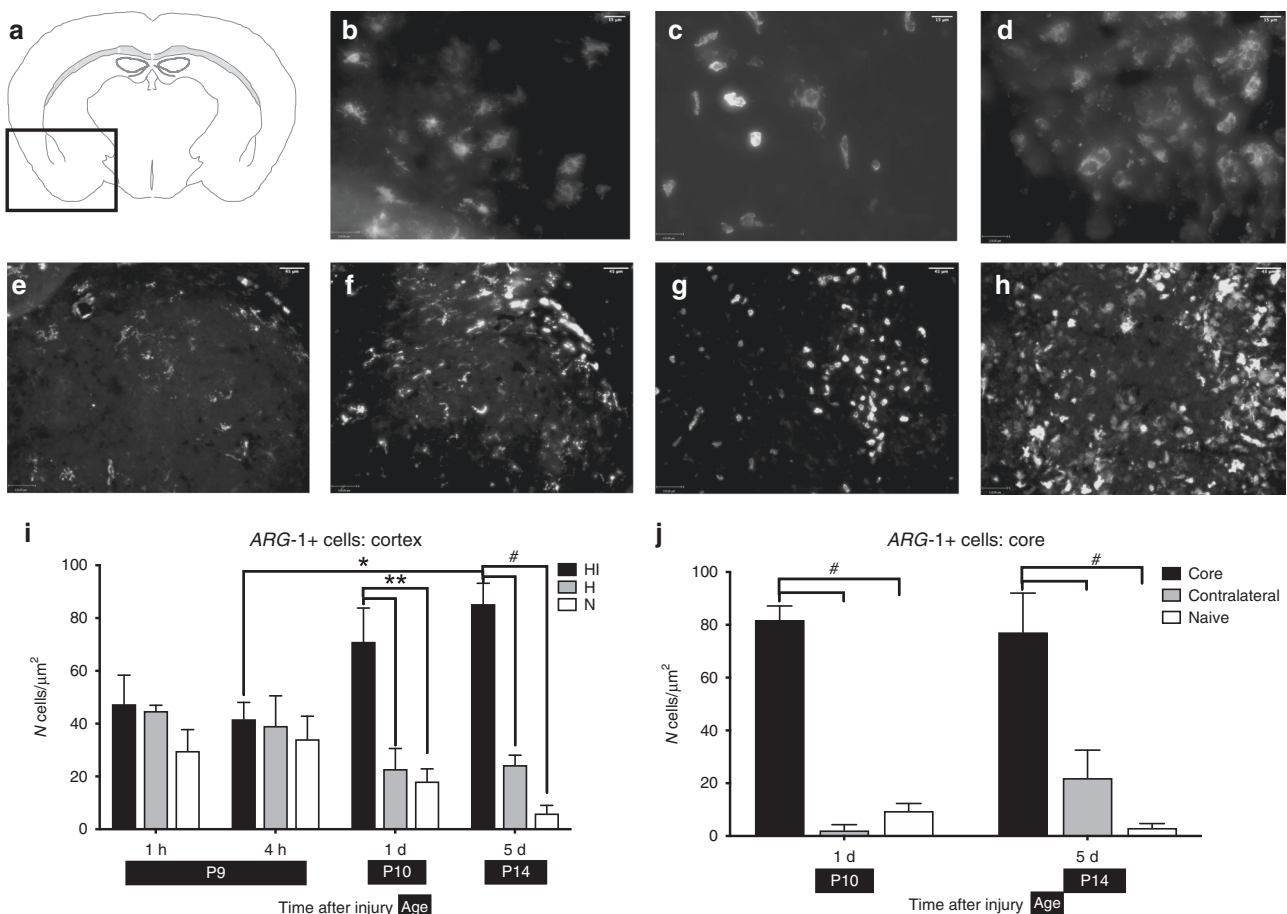


**Fig. 5** Changes in ARG-1<sup>+</sup> microglia after brain HI: **a** anatomical expression of ARG-1 in mice localizes to pyriform cortex, olfactory tubercle, pallidum, striatum, external capsule of corpus callosum, anterior commissure-temporal limb, amygdala, hypothalamus, and caudoputamen. Change in ARG-1<sup>+</sup> microglia morphology as a result of HI from bushy (**b**) into amoeboid (**c**) and round phagocytic (**d**) phenotype. Changes in ARG-1<sup>+</sup> microglia accumulation in the striatum at different timepoints: N mice (**e**), and 4 h (**f**), 1 day (**g**), and 5 days (**h**) after injury. ARG-1<sup>+</sup> microglia count increases in HI cortex (**i**) and HI core in the striatum (**j**) at 1 day after injury, and remains elevated for a prolonged time ( $n = 5-6$  per HI and H group;  $n = 8$  per N group; \* $p < 0.05$ , \*\* $p < 0.01$ , # $p < 0.0001$ ).

detected increase in ARG-2 expression from P9 to P17 in neurons. There is no previous data on ARG-2 expression during P9-P17 in both the hippocampus and the cortex, and while previous studies did not detect ARG-2 increase E13-P1, they did so in adulthood.<sup>20</sup>

Currently, it is not possible to correlate isoform-specific expression to activity as available kits do not differentiate between ARG-1 and ARG-2. This may be why we failed to detect significant changes in ARG activity despite an obvious increase in microglial ARG-1 expression in the cortex. Alternatively, it is possible that ARG-1<sup>+</sup> microglia represent only a small fraction of the expressed ARG-1. Hippocampal activity however is most likely related to ARG-2 expression as this is the predominant isoform expressed in the hippocampus. In our study, ARG activity did not change significantly during neurodevelopment in either region at the ages studied (P9, P10, P14), consistent with previous findings.<sup>21</sup> The regional variation in ARG activity across different cortical regions and subregions of the hippocampus has also been described previously.<sup>22,23</sup> These age-, isoform- and region-specific alterations in ARG expression and activity highlight the tightly regulated functions of this enzyme during neurodevelopment.

Both hypoxia and ischemia-reperfusion injury have been described as a potent stimulus for ARG-1 and ARG-2 expression,<sup>25</sup> and consistent with this, we detected a peak in ARG-1 and ARG-2 expression in the H cortex 5 days after the injury, similar to that reported for ARG-1 by Hamzei et al.<sup>26</sup> Current data on the extent of HI vs. H stimulus on ARG isoform expression are limited and we

speculate that H could be a more potent activator of ARG isoforms than HI, especially in uninjured regions. However, 8 days after the injury we see suppression of ARG-1 and ARG-2 expression in the hippocampus. A similar transient upregulation followed by suppression of ARG-1 was reported by Quirié et al.<sup>27</sup> in an adult rat photothrombotic stroke model at 15 days after the injury. It is possible that the variation in timeline of expression between our studies is related to the age, model, and species studied and suppression of ARG isoforms may be related to the presence of endogenous inhibitors. Cellular localization of ARG was isoform specific, confined to certain anatomical areas, and changed during development and with injury. Notably, we found ARG-1<sup>+</sup> microglia in specific regions of the ventral forebrain and midbrain. A unique population of ARG-1<sup>+</sup> microglia has been shown to represent only 0.5% of microglia formed at E14.5/P4/5, with higher specificity for females.<sup>28</sup> It is possible that ARG-1<sup>+</sup> microglia play role in neurodevelopment and/or sex-specific response to injury.<sup>29</sup> ARG-1<sup>+</sup> microglia have been widely reported after HI injury<sup>30</sup> and are thought to mediate neuroprotective effects. While we detected similarly high numbers of ARG-1<sup>+</sup> microglia at the injury site, not all microglia at the injury site were ARG-1<sup>+</sup>. This dimorphic expression could relate to the origin of the microglia or to the reported microglial "switch" that can happen at the injury site.<sup>31</sup> Interestingly, despite significant evident injury in the hippocampus, ARG-1<sup>+</sup>Iba1<sup>+</sup> cells were only minimally present in this area compared to the injured cortex where ARG-1<sup>+</sup>Iba1<sup>+</sup> were

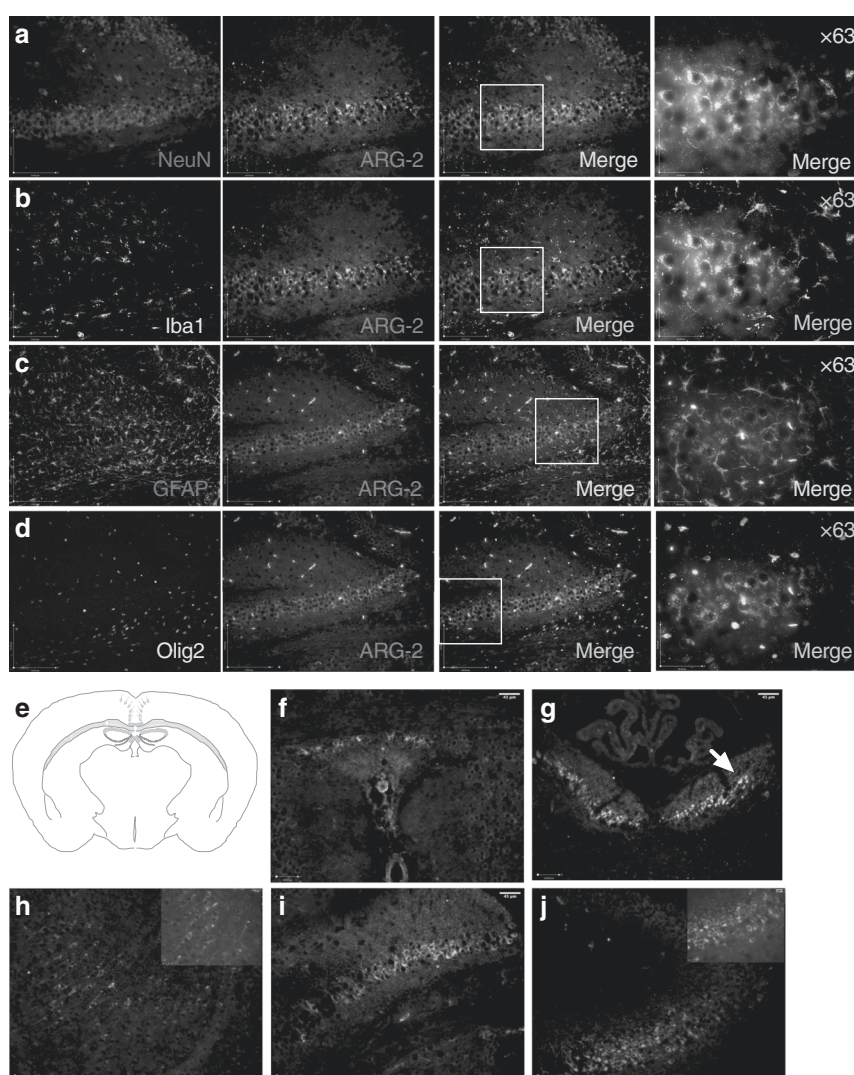


**Fig. 6 Cellular and anatomical expression of ARG-2.** Images of double immunofluorescent staining with ARG-2 antibody (green, middle panels) paired with an antibody specific for neuron (a: NeuN, red panel), microglia (b: Iba1, cyan panel), astrocyte (c: GFAP, red panel), and oligodendrocyte (d: Olig2, cyan panel). Image x63 captures region denoted by a box in the third image of that row. ARG-2 colocalized with NeuN<sup>+</sup> cells (a). Anatomical localization of ARG-2 (e): ARG-2 was found in indusium griseum (f), fasciola cinerea (g), neurons of the neocortex (h), hippocampus CA1 (i), and CA2 (j). Note the pyknotic cells in the HI hemisphere (arrow);  $n = 5-6$  per H and HI group,  $n = 8$  per N group.

detectable as early as 4 h after the injury and persisted for 5 days. This finding demonstrates the heterogeneity of regional responses to injury processes and confirms that injury, protection and recovery mechanisms after injury are modulated in a spatiotemporal fashion. Despite evidence for ARG-1 expression in astrocytes along with neurons and microglia after injury,<sup>25,26</sup> we failed to detect colocalization with GFAP. It is possible that differences in ARG expression and activity during development are based on species, timing after the injury, and injury type.<sup>25,26</sup>

ARG-2 belongs to a group of less studied enzymes in the brain and there are currently few reports on its expression, during neurodevelopment and particularly after injury, in the developing brain. Our findings suggest that this isoform may have roles that are distinct to those of ARG-1, as is evident from the altered cellular and anatomical expression in the brain. Our study is the first to describe ARG-2 expression in structures such as the indusium griseum, fasciola cinerea, or hippocampus. These structures create a continuum referred to as hippocampal rudiments.<sup>32,33</sup> A few neurons expressing ARG-2 were found also in the M1 part of the neocortex. Although the exact function of hippocampal rudiments structures is not well known, they are

believed to play an important role in axonal guidance across the midline during development of brain commissures and interhemispheric connections.<sup>34</sup> The damage of these structures during HI may lead to a spectrum of neurodevelopmental conditions.<sup>35</sup> Expression of ARG-2 in hippocampal rudiments suggests important roles for ARG-2 in mediating at least some of these functions. The presence of ARG-2<sup>+</sup> NeuN<sup>+</sup> cells in the CA1, CA2 of the hippocampus also associates this enzyme with processes of learning and memory formation,<sup>36</sup> emotion, neural cell birth,<sup>37</sup> among others. While recent reports indicate that acetylcholine, dopamine, noradrenaline, 5-hydroxytryptamine, and GABA neurons innervate the indusium griseum,<sup>38</sup> we speculate ARG-2 to primarily localize to GABA-ergic neurons considering it plays important roles in glutamine synthesis.<sup>39</sup> After HI, we see considerable damage of ARG-2<sup>+</sup> cells in almost all of these areas, potentiating a role for ARG-2 in mediating at least some of the learning, memory, and motor deficits seen after HI,<sup>40</sup> and consequently may present an attractive therapeutic target that needs to be validated carefully.

In summary, expression and activity of ARG enzymes change during neurodevelopment and in response to hypoxic and



hypoxic-ischemic brain injury. As ARG-1 localizes mostly to microglia at the injury site, it is possible that its primary role is mediating neuroinflammatory processes. ARG-2 expression, on the other hand, is largely neuronal predominantly in neurodevelopmental structures, suggesting involvement in developmental processes. Further studies are needed to elucidate the precise roles of ARG isoforms in neonatal brain hypoxic and hypoxic-ischemic injury.

## ACKNOWLEDGEMENTS

We thank Sandrijn Vanschaik, Jeff Fineman, and Division of Pediatric Critical Care for their help and support. This work was supported by R35- 5R35NS097299 to D.M.F., UCSF Pediatric Critical Care Division, and the Thrasher Research Fund P0530684.

## AUTHOR CONTRIBUTIONS

J.K.M.: Substantial contributions to conception and design, data acquisition, analysis, and interpretation; drafting the article; final approval of the version to be published. P.P.: Substantial contributions to conception and design, data acquisition, analysis, and interpretation; drafting the article; final approval of the version to be published. R.A.S.: Substantial contributions to data acquisition; drafting the article; final approval of the version to be published. D.M.F.: Substantial contributions to conception and design, data acquisition, analysis, and interpretation; drafting the article; final approval of the version to be published.

## ADDITIONAL INFORMATION

**Competing interests:** The material is original, has not been previously published, and has not been submitted for publication elsewhere while under consideration. The authors declare no competing interests.

**Publisher's note** Springer Nature remains neutral with regard to jurisdictional claims in published maps and institutional affiliations.

## REFERENCES

1. LaFemina, M. J., Sheldon, R. A. & Ferriero, D. M. Acute hypoxia-ischemia results in hydrogen peroxide accumulation in neonatal but not adult mouse brain. *Pediatr. Res.* **59**, 680–683 (2006).
2. Choi, S., Park, C., Ahn, M., Lee, J. H. & Shin, T. Immunohistochemical study of arginase 1 and 2 in various tissues of rats. *Acta Histochem.* **114**, 487–494 (2012).
3. Handley, R. R. et al. Brain urea increase is an early Huntington's disease pathogenic event observed in a prodromal transgenic sheep model and HD cases. *Proc. Natl Acad. Sci. USA* **114**, E11293–E11302 (2017).
4. Villalba, N. et al. Traumatic brain injury causes endothelial dysfunction in the systemic microcirculation through arginase-1-dependent uncoupling of endothelial nitric oxide synthase. *J. Neurotrauma* **34**, 192–203 (2017).
5. Ahn, M. et al. Immunohistochemical study of arginase-1 in the spinal cords of Lewis rats with experimental autoimmune encephalomyelitis. *Brain Res.* **1453**, 77–86 (2012).
6. Petrone, A. B. et al. The role of arginase 1 in post-stroke immunosuppression and ischemic stroke severity. *Transl. Stroke Res.* **7**, 103–110 (2016).
7. Morris, S. & Wu, G. Arginase: nitric oxide and beyond. *Biochem. J.* **336**, 1–17 (1998).
8. Nguyen, M. C. et al. Arginase inhibition restores peroxynitrite-induced endothelial dysfunction via L-arginine-dependent endothelial nitric oxide synthase phosphorylation. *Yonsei Med. J.* **57**, 1329–1338 (2016).
9. Estévez, A. G. et al. Arginase 1 regulation of nitric oxide production is key to survival of trophic factor-deprived motor neurons. *J. Neurosci.* **26**, 8512–8516 (2006).
10. Jonathan, D., Cherry, J. D., Olschowka, J. A. & O'Banion, K. M. Neuroinflammation and M2 microglia: the good, the bad, and the inflamed. *J. Neuroinflamm.* **11**, 98 (2014).
11. Cai, D. et al. Arginase I and polyamines act downstream from cyclic AMP in overcoming inhibition of axonal growth MAG and myelin in vitro. *Neuron* **35**, 711–719 (2002).
12. Huang, Y., Higginson, D. S., Hester, L., Park, M. H. & Snyder, S. H. Neuronal growth and survival mediated by eIF5A, a polyamine-modified translation initiation factor. *Proc. Natl Acad. Sci. USA* **104**, 4194–4199 (2007).
13. Deng, K. et al. Increased synthesis of spermidine as a result of upregulation of arginase I promotes axonal regeneration in culture and in vivo. *J. Neurosci.* **29**, 9545–9552 (2009).

14. Alizadeh, A. et al. Neuregulin-1 positively modulates glial response and improves neurological recovery following traumatic spinal cord injury. *Glia* **65**, 1152–1175 (2017).
15. Krystofova, J., Pathipati, P., Russ, J., Sheldon, A. & Ferriero, D. The arginase pathway in neonatal brain hypoxia-ischemia. *Dev. Neurosci.* **17**, 1–14 (2019).
16. Yu, H. et al. Arginase expression in mouse embryonic development. *Mech. Dev.* **115**, 151–155 (2002).
17. Grillo, M. A., Fossa, T. & Dianzani, U. Arginase, ornithine decarboxylase and Sadenosylmethionine decarboxylase in chicken brain and retina. *Int. J. Biochem.* **15**, 1081–1084 (1983).
18. Liu, P., Smith, P., Appleton, I., Darlington, C. & Bilkey, D. Age-related changes in nitric oxide synthase and arginase in the rat prefrontal cortex. *Neurobiol. Aging* **25**, 547–552 (2004).
19. Crain, J. M., Nikodemova, M. & Watters, J. J. Microglia express distinct M1 and M2 phenotypic markers in the postnatal and adult central nervous system in male and female mice. *J. Neurosci. Res.* **91**, 1143–1151 (2013).
20. Yu, H. et al. Expression of arginase isozymes in mouse brain. *J. Neurosci. Res.* **66**, 406–422 (2001).
21. Konarska, L. & Tomaszewski, L. Studies on L-arginase in developing rat small intestine, brain, and kidney. I. Ontogenic evolution of arginase isoenzymes. *Biochem. Med. Metab. Biol.* **35**, 156–169 (1986).
22. Liu, P., Smith, P. F., Appleton, I., Darlington, C. L. & Bilkey, D. K. Regional variations and age-related changes in nitric oxide synthase and arginase in the sub-regions of the hippocampus. *Neuroscience* **119**, 679–687 (2003).
23. Liu, P., Smith, P. F., Appleton, I., Darlington, C. L. & Bilkey, D. K. Nitric oxide synthase and arginase in the rat hippocampus and the entorhinal, perirhinal, postnatal, and temporal cortices: regional variations and age-related changes. *Hippocampus* **13**, 859–867 (2003).
24. © 2004 Allen Institute for Brain Science. *Allen Mouse Brain Atlas* <https://mouse.brain-map.org>.
25. Shosha, E. et al. Arginase 2 promotes neurovascular degeneration during ischemia/reperfusion injury. *Cell Death Dis.* **7**, e2483 (2016).
26. Hamzei Taj, S., Kho, W., Riou, A., Wiedermann, D. & Hoehn, M. MiRNA-124 induces neuroprotection and functional improvement after focal cerebral ischemia. *Bio-materials* **91**, 151–165 (2016).
27. Quirié, A. et al. Effect of stroke on arginase expression and localization in the rat brain. *Eur. J. Neurosci.* **37**, 1193–1202 (2013).
28. Hammond, T. R. et al. Single-cell RNA sequencing of microglia throughout the mouse lifespan and in the injured brain reveals complex cell-state changes. *Immunity* **50**, 253–271.e6 (2019).
29. Lee, S. et al. Abstract TP507: sex-related differences in neonatal stroke: International Maternal Newborn Stroke Registry. *Stroke* **50**, ATP507–ATP507 (2019).
30. Hellström Erkenstam, N. et al. Temporal characterization of microglia/macrophage phenotypes in a mouse model of neonatal hypoxic-ischemic brain injury. *Front. Cell Neurosci.* **10**, 286 (2016).
31. Fumagalli, S., Perego, C., Pischiutta, F., Zanier, E. R. & De Simoni, M. G. The ischemic environment drives microglia and macrophage function. *Front. Neurol.* **6**, 1–19 (2015).
32. Carpenter, M. B. *Human Neuroanatomy* 7th edn, 532pp (Williams and Wilkins, Baltimore, 1976).
33. Adamek, G. D., Shipley, M. T. & Sanders, M. S. The indusium griseum in the mouse: architecture, Timm's histochemistry and some afferent connections. *Brain Res. Bull.* **12**, 657–668 (1984).
34. Morcom, L. R., Edwards, T. J., Richards, L. J. *Chapter 14—Cortical Architecture, Midline Guidance, and Tractography of 3D White Matter Tracts. Axons and Brain Architecture* 289–313 (Academic Press, 2016).
35. Paul, L. K. et al. Agenesis of the corpus callosum: genetic, developmental and functional aspects of connectivity. *Nat. Rev. Neurosci.* **8**, 287–299 (2007).
36. Bendel, O. et al. Reappearance of hippocampal CA1 neurons after ischemia is associated with recovery of learning and memory. *J. Cereb. Blood Flow. Metab.* **25**, 1586–1595 (2005).
37. Gulyaeva, N. Functional neurochemistry of the ventral and dorsal hippocampus: stress, depression, dementia and remote hippocampal damage. *Neurochem. Res.* **44**, 1306–1322 (2019).
38. Di Ieva, A., Fathalla, H., Cusimano, M. D. & Tschabitscher, M. The indusium griseum and the longitudinal stria of corpus callosum. *Cortex* **62**, 34–40 (2015).
39. Li, H. et al. Regulatory role of arginase I and II in nitric oxide, polyamine, and proline syntheses in endothelial cells. *Am. J. Physiol. Metab.* **280**, E75–E82 (2001).
40. Martinez-Biarge, M., Ferriero, D. & Cowan, F. M. Perinatal arterial ischemic stroke. *Handb. Clin. Neurol.* **162**, 239–266 (2019).